Cation Distribution Study of Al^{3+} Doped Zn-Ni-Cu Ferrite

B. L. Shinde

Assistant Professor
Department of Chemistry, Waghire College, Saswad,
Dist: Pune, 412301 (M.S.) India

ABSTRACT: Al^{3+} doped Zn-Ni-Cu ferrites prepared by the wet chemical co-precipitation method. The cation distribution determined using Bertaut method. The XRD patterns confirmed the formation of cubic spinel structure of single phase ferrites. In the Al^{3+} doped Zn-Ni-Cu ferrite system Zn^{2+} ions occupy the tetrahedral site (A sublattice) and both Ni^{2+} and Cu^{2+} ions enter octahedral site (B sublattice), while, Fe^{3+} ions occupy both the available tetrahedral (A) and octahedral [B] sublattices. Al^{3+} ions predominately occupy the octahedral sites. With increasing Al^{3+} content, the fraction Al^{3+} ions in octahedral sites increases, whereas the fraction of Fe^{3+} ions in octahedral sites decreases linearly. The value of the oxygen positional parameter 'u' increased and theoretical lattice constant decreased with Al^{3+} substitution. The tetrahedral edge and shared and unshared octahedral edges decrease with Al^{3+} substitution.

Index Terms **– Cation distribution, Zn-Ni-Cu Ferrite, XRD.**

I. INTRODUCTION

Spinel ferrites were generally used in various electronic and magnetic devices due to their high magnetic permeability and low magnetic losses [1]. They have large range of technological applications in transformer cores, inductors, high quality filters, radio frequency circuits, etc. [2-3]. Recently, Zn-Ni-Cu ferrites have been the leading materials for multilayer ferrite chip inductor [4]. The site occupancy is often depicted in the chemical formula as $(M_{1-\delta}Fe_{\delta})[M_{\delta}\ Fe_{2-\delta}]O_4$, where round and square brackets denote the A- and B-sites, respectively, M represents a metal cation, and 'δ' is the inversion parameter. The degree of inversion 'δ' for spinel ferrites are defined as the fraction of tetrahedral (A)-sites occupied by trivalent cations. Accordingly, for a normal spinel δ = 0 and for a completely inverse spinel, δ = 1. In the normal spinel ferrites MFe_2O_4, the divalent ions are all in 'A' sites and the Fe^{3+} ions occupy 'B' sites. In spinel structure the magnetic ions are distributed among two different lattices, tetrahedral (A) and octahedral (B) sites and are ordered antiparallel to each other cubic spinel ferrites has two sub lattices: Tetrahedral (A) site and Octahedral (B) site in AB_2O_4 crystal structure [5-6]. The important structural, electrical and magnetic properties of spinels, responsible for their application in various fields are found to depend on the distribution of cations among to depend on the distribution of cations among the sites [7]. Therefore the estimation of the cation distribution turns out to be important. Various cations can be replaced in A site and B site to tune its magnetic properties. In Zn-Ni-Cu ferrites due to the favorable fit of charge distribution, Ni^{2+} and Cu^{2+} ions show strong preference to B sites. Zn^{2+} ions show a strong preference for A-sites due to its electronic configuration [8-9]. In this paper, a cationic distribution studies $Zn_{0.6}Cu_{0.2}Ni_{0.2}Fe_{2-x}Al_xO_4$ ferrites with composition (x = 0.0, 0.2, 0.4, 0.6, 0.8 and 1.0) derived by the wet chemical co-precipitation method were reported.

II. EXPERIMENTAL

$Zn_{0.6}Cu_{0.2}Ni_{0.2}Fe_{2-x}Al_xO_4$ ferrites with composition (x = 0.0, 0.2, 0.4, 0.6, 0.8 and 1.0) derived by the wet chemical co-precipitation method [10]. The metal sulphates solution prepared by dissolving metal sulphates in desired composition in deionized water to yield clear solution; the initial pH of solution was 3. The 2M NaOH solution used as precipitant, in oxygen atmosphere at 80 ^{O}C, temperature, brownish precipitate of precursor obtained when pH of solution becomes 12. The precipitate was filtered, washed with deionized water till free from sodium sulphates and then dried. Prepared precursors were sintered at 600 °C for 4 hour to obtain the spinel ferrites.

Characterization*:*

X-ray powder diffraction studied by Phillips X-ray diffractometer (Model 3710). Morphology of the powder samples were studied on JEOL-JSM-5600 N Scanning Electron Microscope. The infrared spectra of all the samples were recorded in the range 200 to 800 cm^{-1} using Perkin Elmer infrared spectrophotometer. Morphology of the powder samples were studied on JEOL-JSM-5600 N Scanning Electron Microscope (SEM).

III. RESULTS AND DISCUSSION:

Typical X-ray diffraction (XRD) patterns of the Al^{3+} Doped Zn-Ni-Cu ferrite system are shown in Figure 1. The XRD patterns confirmed the formation of cubic spinel structure of single phase ferrites. Lattice constant (a), x-ray density and crystallite size of all the samples was determined [10], Lattice constant (a), x-ray density and crystallite size decreases with increase in Al^{3+} composition.

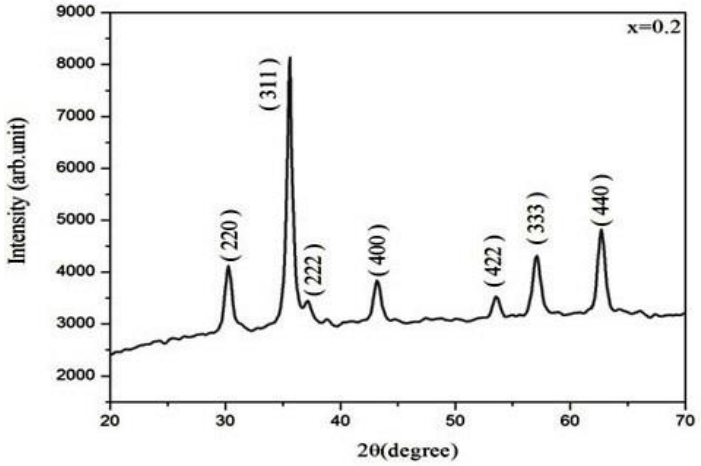

Figure 1: Typical XRD pattern for samples x =0.2

Typical IR spectra of the chromium Al^{3+} Doped Zn-Ni-Cu ferrite system is shown in Figure 2.

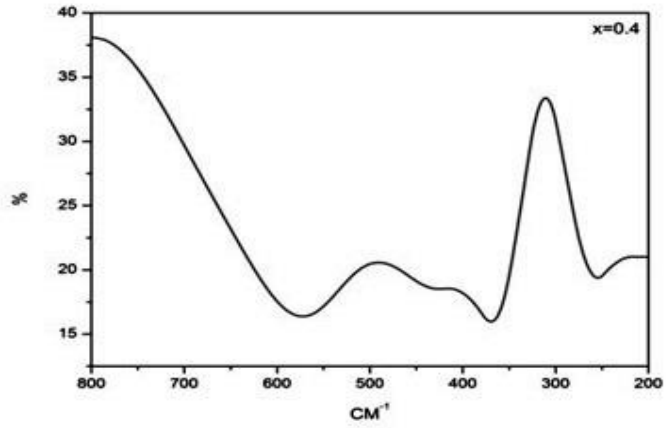

Figure 2: Typical IR spectrum for samples x =0.4

It is observed from figure that the higher frequency band (ν_1) is appeared in the range of 560 - 595 cm^{-1} assigned to tetrahedral site whereas lower frequency band (ν_2) is appeared in the range of 430 - 450 cm^{-1} assigned to octahedral site. These bands are characteristics features of spinel structure.

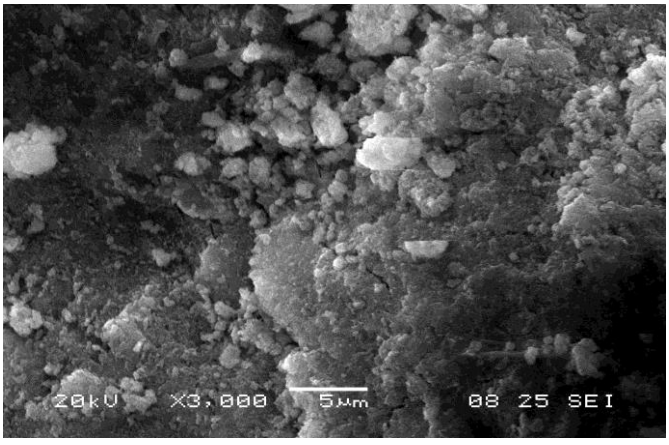

Figure 3: Scanning electron micrograph for sample x = 0.2

Typical Scanning electron micrograph (SEM) of the surfaces of the Al^{3+} Doped Zn-Ni-Cu ferrite system is shown in Figure 3. It is observed from the SEM image that the prepared samples are amorphous and porous in nature.

CATION DISTRIBUTION:

The cation distribution in spinel ferrite can be obtained from an analysis of the X-ray diffraction pattern. In the present work, the Bertaut method [11] is used to determine the cation distribution. The cation distribution is achieved by comparing the experimental and calculated intensity ratios for reflections whose intensities (i) are nearly independent of the oxygen parameter, (ii) vary with the cation distribution in opposite ways and (iii) do not significantly differ. In the present work the ratio of (220)/(440) and (422)/(440) were used. The ratios of these planes are sensitive to cation distribution and are listed in Table 1. The cation distribution for each concentration and the site preferences of cations distributed among the tetrahedral (A) and octahedral [B] sites are listed in Table 1. One can find the Zn^{2+} ions prefer to occupy the tetrahedron site (A sublattice) and both Ni^{2+} and

Cu^{2+} ions mainly enter octahedron site (B sublattice). However, Fe^{3+} ions occupy both the available tetrahedral (A) and octahedral [B] sublattices. Al^{3+} preferentially replaces Fe^{3+} from octahedral sites because of favorable crystal field effects ($Al^{3+}6/5\Delta_0$, $Al^{3+}0\Delta_0$) [11]. The data in Table 1 show that Al^{3+} ions predominately occupy the octahedral sites, which is consistent with the preference for large octahedral site energy. With increasing Al^{3+} content, the fraction Al^{3+} ions in octahedral sites increases, whereas the fraction of Fe^{3+} ions in octahedral sites decreases linearly.

The mean ionic radius of the tetrahedral A- and octahedral B-sites (r_A and r_B) was calculated [12, 13]. It is observed that radius of tetrahedral site 'r_A' remains constant at (0.712 Å) whereas radius of octahedral site 'r_B' decreases with increasing Al^{3+} substitution (Table 2). The decrease in r_B is due to the increasingly high occupation of the B site by the smaller ionic radius of Al^{3+} (0.53 Å) ions that replacing Fe^{3+} (0.67 Å) ions.

Table 1:Cation distribution and Intensity ratios

Comp. **'x'**	**Cation distribution**	**Intensity ratio**			
		$I_{(220)}/I_{(400)}$		$I_{(422)}/I_{(440)}$	
		Cal.	**Obs.**	**Cal.**	**Obs.**
0.0	$(Zn_{0.6}Fe_{0.4})$ $(Ni_{0.2}Cu_{0.2}Fe_{1.6})$	1.7568	1.0994	0.2716	0.7266
0.2	$(Zn_{0.6}Fe_{0.4})$ $(Ni_{0.2}Cu_{0.2}Fe_{1.4}Al_{0.2})$	1.9262	1.0682	0.3002	0.7360
0.4	$(Zn_{0.6}Fe_{0.4})$ $(Ni_{0.2}Cu_{0.2}Fe_{1.2}Al_{0.4})$	2.1848	1.0669	0.3008	0.7360
0.6	$(Zn_{0.6}Fe_{0.4})$ $(Ni_{0.2}Cu_{0.2}Fe_{1.0}Al_{0.6})$	2.4180	1.1052	0.3152	0.8176
0.8	$(Zn_{0.6}Fe_{0.4})$ $(Ni_{0.2}Cu_{0.2}Fe_{0.8}Al_{0.8})$	2.7623	1.1406	0.3344	0.7809
1.0	$(Zn_{0.6}Fe_{0.4})$ $(Ni_{0.2}Cu_{0.2}Fe_{0.6}Al_{1.0})$	3.1637	1.0238	0.3554	0.7956

The theoretical values of lattice constant (a_{th}) were calculated by following equation [14]:

$$a_{th} = \frac{8}{3}\sqrt{3}\left[(r_A + R_0) + \sqrt{3}(r_B + R_0)\right] \quad (1)$$

where r_A and r_B are radii of tetrahedral (A) site and octahedral [B] site, R_O is radius of oxygen ion (1.32 Å). The values of the theoretical lattice parameters for the different substitution level of Al^{3+} ions is given in Table 2 and its variation is shown in Figure 7. The theoretical lattice constant decreased from 8.4618 Å (x = 0.0) to 8.2351 Å (x = 1.0) with the Al^{3+} substitution.

The oxygen positional parameter '*u*' was calculated using the following equation [14]:

$$u = \left[(r_A + R_0)\frac{1}{\sqrt{3}a} + \frac{1}{4}\right] \quad (2)$$

where 'a' is lattice constant, 'R_O' is the radius of oxygen ion (1.32 Å) and 'r_A' is the radius of tetrahedral A-site. In most oxidic spinels the oxygen ions are apparently larger than the metallic ions, and in spinel like structure the oxygen parameter has a value of about 0.375 for which the arrangement of O^{2-} ions equals exactly a cubic closed packing, but in actual spinel lattice this ideal pattern is slightly deformed. For a given spinel compound, the anion sublattice expands or contracts on varying oxygen parameter until the tetrahedral and the octahedral site volumes match the radii of the constituent cations. As observed from Table 2 that the u increased from 0.3832 Å to 0.3889 Å with the substitution of Al^{3+} ions in NiCuZn ferrite. Little higher value of obtained u is due to a small displacement of the anions with the expansion of the tetrahedral interstices 'r_A'.

Table 2: Lattice Ionic radii r_A and r_B and theoretically lattice constant of system

Composition 'x'	r_A (Å)	r_B (Å)	a_{th} (Å)	u (Å)
0.0	0.712	0.68	8.4618	0.3832
0.2	0.712	0.663	8.4165	0.3875
0.4	0.712	0.646	8.3711	0.3878
0.6	0.712	0.629	8.3258	0.3884
0.8	0.712	0.612	8.2805	0.3887
1.0	0.712	0.595	8.2351	0.3889

The allied parameters such as tetrahedral and octahedral bond length (d_{Ax} and d_{Bx}), tetrahedral edge, shared and unshared octahedral edge (d_{AXE}, d_{BXE} and d_{BXEU}) were calculated:

$$d_{AX} = a\sqrt{3}\left(u - \frac{1}{4}\right) \quad (3)$$

$$d_{BX} = a\left[3u^2 - \left(\frac{11}{4}\right)u + \frac{43}{64}\right]^{\frac{1}{2}} \quad (4)$$

$$d_{AXE} = a\sqrt{2}\left(2u - \frac{1}{2}\right) \quad (5)$$

$$d_{BXEshaired} = a\sqrt{2}\left(1 - 2u\right) \quad (6)$$

$$d_{BXEunshaied} = a\left(4u^2 - 3u + \frac{11}{16}\right)^{\frac{1}{2}} \quad (7)$$

where '*a*' is the experimental values of lattice constant and 'u' is oxygen positional parameter.

The values are presented in Table 3, which indicates that the tetrahedral and octahedral bond lengths decreases as Al^{3+} ion substitution increases. The tetrahedral edge and shared and unshared octahedral edges decrease with Al^{3+} substitution and may be due to the comparatively smaller ionic radii of Al^{3+} as compared to Fe^{3+} ions.

Table 3: Tetrahedral Bond (d_{AX}), Octahedral Bond (d_{BX}), Tetra Edge (d_{AXE}) and Octa Edge (d_{BXE})

Composition 'x'	d_{AX} (Å)	d_{BX} (Å)	Edges		
			Tetra edge (Å)	Octa edge d_{BXE} (Å)	
			d_{AXE}	Shared	Unshared
0.0	1.9148	2.0603	3.1267	2.8403	2.9852
0.2	1.9001	2.0444	3.1027	2.8185	2.9623
0.4	1.8940	2.0379	3.0867	2.8040	2.9528
0.6	1.8906	2.0342	3.0872	2.8044	2.9475
0.8	1.8903	2.0339	3.0927	2.8094	2.9470
1.0	1.8903	2.0339	3.0867	2.8040	2.9470

IV. CONCLUSION:

Al^{3+} doped Zn-Ni-Cu ferrites prepared by the by the wet chemical co-precipitation method. In the $Zn_{0.6}Cu_{0.2}Ni_{0.2}Fe_{2-x}Al_xO_4$ system Zn^{2+} ions occupy the tetrahedral site (A sublattice) and both Ni^{2+} and Cu^{2+} ions mainly enter octahedral site (B sublattice), while, Fe^{3+} ions occupy both the available tetrahedral (A) and octahedral [B] sublattices. Al^{3+} ions predominately occupy the octahedral sites. With increasing Al^{3+} content, the fraction Al^{3+} ions in octahedral sites increases, whereas the fraction of Fe^{3+} ions in octahedral sites decreases linearly. The value of the oxygen positional parameter 'u' increased and theoretical lattice constant decreased with Al^{3+} substitution. The tetrahedral edge and shared and unshared octahedral edges decrease with Al^{3+} substitution.

V. REFERENCES:

[1] Suzuki, T., Tanaka, T. and Ikemizu, K., 2001. High density recording capability for advanced particulate media. *Journal of magnetism and magnetic materials*, *235*(1-3), pp.159-164.

[2] Verma, A., Goel, T.C., Mendiratta, R.G. and Gupta, R.G., 1999. High-resistivity nickel–zinc ferrites by the citrate precursor method. *Journal of magnetism and magnetic materials*, *192*(2), pp.271-276.

[3] Lakshman, A., Rao, K.H. and Mendiratta, R.G., 2002. Magnetic properties of In3+ and Cr3+ substituted Mg–Mn ferrites. *Journal of magnetism and magnetic materials*, *250*, pp.92-97.

[4] Jean, J.H., Lee, C.H. and Kou, W.S., 1999. Effects of Lead (II) Oxide on Processing and Properties of Low-Temperature-Cofirable Ni-Cu-Zn Ferrite. *Journal of the American Ceramic Society*, *82*(2), pp.343-350. [5] Kane, S.N. and Satalkar, M., 2017. Correlation between magnetic properties and cationic distribution of Zn 0.85− x Ni x Mg 0.05 Cu 0.1 Fe 2 O 4 nano spinel ferrite: effect of Ni doping. *Journal of materials science*, *52*(6), pp.3467-3477.

[6] Ramakrishna, K.S., Srinivas, C., Meena, S.S., Tirupanyam, B.V., Bhatt, P., Yusuf, S.M., Prajapat, C.L., Potukuchi, D.M. and Sastry, D.L., 2017. Investigation of cation distribution and magnetocrystalline anisotropy of NixCu0. 1Zn0. 9− xFe2O4 nanoferrites: Role of constant mole percent of Cu2+ dopant in place of Zn2+. *Ceramics International*, *43*(11), pp.7984-7991.

[7] Sun, K., Wu, G., Wang, B., Zhong, Q., Yang, Y., Yu, Z., Wu, C., Wei, P., Jiang, X. and Lan, Z., 2015. Cation distribution and magnetic property of Ti/Sn-substituted manganese–zinc ferrites. *Journal of Alloys and Compounds*, *650*, pp.363-369.

[8] Tehrani, F.S., Daadmehr, V., Rezakhani, A.T., Akbarnejad, R.H. and Gholipour, S., 2012. Structural, magnetic, and optical properties of zinc-and copper-substituted nickel ferrite nanocrystals. *Journal of superconductivity and novel magnetism*, *25*(7), pp.2443-2455.

[9] Gabal, M.A., Al-Thabaiti, S.A., El-Mossalamy, E.H. and Mokhtar, M., 2010. Structural, magnetic and electrical properties of Ga-substituted NiCuZn nanocrystalline ferrite. *Ceramics International*, *36*(4), pp.1339-1346.

[10] Shinde, B.L. and Lohar, K.S., 2017. Evaluation of Microstructure and Magnetic Properties of Aluminium Doped Copper Nickel Zinc Spinel Ferrites. *Infrared spectroscopy*, *4*(11.59), pp.13-15.

[11] Weil, L., Bertaut, F., & Bochirol, L., *Journal de Physique et le Radium*, 1950, *11*(5), 208-212.

[12] Amer, M. A., *Hyperfine interactions*, 2000, *131*(1), 29-42.

[13] Yousif, A. A., Elzain, M. E., Mazen, S. A., Sutherland, H. H., Abdalla, M. H., & Masour, S. F., *Journal of Physics: Condensed Matter*, 1994, *6*(29), 5717.

[14] R. Valenzuela, *Magnetic ceramics*, Cambridge University Press, (1994).